Biological Journal of the Linnean Society, 2019, **128**, 130–137. With 2 figures.

A river runs through it: tree frog genomics supports the Dead Sea Rift as a rare phylogeographical break

CHRISTOPHE DUFRESNES[1*], GLIB MAZEPA[2,3], DANIEL JABLONSKI[4], RIYAD A. SADEK[5] and SPARTAK N. LITVINCHUK[6,7]

[1]*Laboratory for Conservation Biology, University of Lausanne, Biophore Building, 1015 Lausanne, Switzerland*
[2]*Department of Ecology & Evolution, University of Lausanne, Biophore Building, 1015 Lausanne, Switzerland*
[3]*Department of Ecology and Genetics, Evolutionary Biology, Norbyvägen 18D, 75236 Uppsala, Sweden*
[4]*Department of Zoology, Comenius University in Bratislava, Ilkovičova 6, Mlynská dolina, 842 15 Bratislava, Slovakia*
[5]*Biology Department, American University of Beirut, Bliss Street, 1107 2020, Beirut, Lebanon*
[6]*Institute of Cytology, Russian Academy of Sciences, Tikhoretsky pr. 4, St. Petersburg 194064, Russia*
[7]*Department of Zoology and Physiology, Dagestan State University, Gadzhiyev str. 43-a, Makhachkala, Dagestan, 3367000, Russia*

Received 17 March 2019; revised 30 April 2019; accepted for publication 30 April 2019

Phylogeographical breaks can be viewed as regional hotspots of diversity where the genetic integrity of incipient species is put to the test. We focus on an understudied species transition from the Middle East, namely the Dead Sea Rift in the Levant region, which presumably divided the tree frogs *Hyla savignyi* and *H. felixarabica*. Combining multilocus genetic analyses (mitochondrial DNA and RAD-sequencing) with ecological niche modelling, we test whether the rift effectively acts as a biogeographical barrier preventing this pair from admixing and merging. The answer is yes: despite weak signs of introgression, all parapatric populations were assigned to either species without cyto-nuclear discordance. Yet, the projected distributions under present and glacial conditions largely overlapped in the area, meaning their current parapatric ranges do not represent an ecological transition. Instead, we hypothesize that *H. savignyi* and *H. felixarabica* are maintained apart by limited opportunities for dispersal across the barren Jordan Valley, combined with advanced reproductive isolation. Therefore, the Dead Sea Rift may represent a rare phylogeographical break, and we encourage international efforts to assess its contribution to the rich biodiversity of the Middle East.

ADDITIONAL KEYWORDS: amphibians – biodiversity – biogeography – *Hyla felixarabica* – *Hyla savignyi* – Levant – RAD-sequencing – speciation.

INTRODUCTION

Phylogeographical breaks can promote regional hotspots of biodiversity, where diverging lineages meet and are maintained apart through demographic, ecological and/or genetic processes (Hewitt, 2011). Geographical transitions between reproductively isolated pairs of species are particularly important, especially when they are shared across different species assemblages, i.e. 'suture zones' (Remington, 1968). Documenting these transitions requires analyses of allo- and parapatric populations in candidate regions to test whether the interacting taxa have maintained their genetic integrity despite opportunities for gene flow.

The Levant, which broadly encompasses Cyprus, Israel, Jordan, West Bank, Lebanon, Syria and southern Turkey (Hatay Province), is a biogeographical crossroads between European, African and Asian biota. This region is known for its great geological and climatic instability since the Late Miocene (Heller, 2007). In particular, collisions between the Arabian, Anatolian

*Corresponding author. E-mail: Christophe.Dufresnes@hotmail.fr

and African tectonic plates led to the formation of the Dead Sea Rift, a series of faults running from the Red Sea to Anatolia, which disconnected populations into separate basins. This is best exemplified by *Latonia nigriventer*, a famously rediscovered amphibian endemic to the Hula Valley in Israel (Biton et al., 2013). The progressive aridification of the Eastern Mediterranean region during the Pliocene (Schuster *et al.*, 2006) further contributed to isolate evolutionary lineages in allopatric shelters (Tamar *et al.*, 2015), while the subsequent climatic oscillations of the Pleistocene provided some opportunities for biotic exchanges (Heller, 2007). Today, the Dead Sea Rift marks the boundary to the distribution of Levantine lineages in several terrestrial vertebrates (Gvoždík *et al.*, 2010; Kornilios *et al.*, 2012, 2017; Ahmadzadeh *et al.*, 2013; Poulakakis *et al.*, 2013; Tamar *et al.*, 2015; Baier *et al.*, 2017; Jandzik *et al.*, 2018). This potential barrier is particularly relevant for ecthotermic species such as herpetofauna, as it separates the Mediterranean habitats of the Levantine coast from the dry deserts of Syria and Jordan.

Tree frogs (Hylidae) make an adequate model to study this transition. Based on mitochondrial DNA (mtDNA) and two short intronic sequences, Gvoždík *et al.* (2010) mapped the distribution of two Middle Eastern taxa parapatric along the Dead Sea Rift, namely *Hyla savignyi* on the coast of Israel, Lebanon and south-western Anatolia, and the Levant clade of *Hyla felixarabica* across Jordan and Syria (considered synonyms by some authors, e.g. Degani *et al.*, 2012). Signs of hybridization (syntopy of mitotypes and co-segregation of species-diagnostic alleles at intron markers) were found in a single locality of the Hula valley, close to the Lebanon–Israel border (Gvoždík *et al.*, 2010), suggesting their genomes are still permeable to gene flow despite Miocene divergence (8.5–4.4 Mya, based on genome-wide RAD-data, Dufresnes *et al.*, 2018). *Hyla* species of similar age may show either reduced (e.g. *H. arborea* and *H. orientalis*) or widespread introgression across secondary contact zones (e.g. *H. arborea* and *H. molleri*) (Dufresnes *et al.*, 2018, and references therein). In this group, contacts may be partially mediated by ecological divergence at environmental transitions (e.g. *H. intermedia* and *H. perrini*, Dufresnes *et al.*, 2018). Assessing which scenario prevails between *H. savignyi* and *H. felixarabica* will, by extension, provide insights into the putative role played by the Dead Sea Rift in shaping their diversity and distributions.

Here, we report such assessment by combining genomic analysis of *H. savignyi* and *H. felixarabica* along the Dead Sea Rift with past and present species distribution modelling. Our objectives were (1) to measure genetic admixture in parapatric populations and (2) to gain insight into whether the rift represents an ecological transition for tree frogs.

MATERIAL AND METHODS

Sampling and laboratory procedures

Tissue samples were collected from wild-caught adults or larvae and stored in 70–96% ethanol. A total of 77 individuals were included from 11 Levantine localities (Israel, Jordan and Lebanon), as well as three from Cyprus. Full details can be found in Supporting Information Table S1. DNA was extracted using the Qiagen Robotic Workstation.

To mitotype our samples, we amplified, sequenced and aligned ~500 bp of the mitochondrial 16S rRNA gene (16S) in 68 individuals, as described by Dufresnes *et al.* (2019b). Two additional samples yielded shorter sequences sufficient for species barcoding (but excluded from the genetic analyses described below). We genotyped thousands of loci in 54 samples (Supporting Information, Table S1) by preparing and sequencing a genomic library of double-digested RAD (ddRAD) loci following the ad hoc protocol of Brelsford *et al.* (2016). We used enzymes *Sbf*I and *Msp*I, a size-selection of 400–500 bp, and sequenced the pooled, barcoded fragments on one lane of an Illumina HiSeq 2500 (single read 125 bp). We then followed the same bioinformatic pipeline as in Dufresnes *et al.* (2018b) for demultiplexing and cataloguing reads with Stacks 1.48 (Catchen *et al.*, 2013). We called single nucleotide polymorphisms (SNPs) present in all samples of all populations, and obtained a genotype matrix of 1472 SNPs.

Genetic analyses

We combined our 68 mtDNA sequences (16S) with 38 homologous sequences from the two species published by Gvoždík *et al.* (2010). First, we built a haplotype network based on these 106 sequences (TCS, Clement *et al.*, 2000). Second, we performed a maximum-likelihood phylogenetic reconstruction of the 43 unique haplotypes identified among these sequences using PhyML 3.2 (Guidon *et al.*, 2010), with a GTR+G model of sequence evolution (Gvoždík *et al.*, 2010) and 1000 bootstrap replicates. *Hyla meridionalis* was used as outgroup (GenBank accession KF956382). The distribution of the mtDNA lineages in the Levant region was completed with the addition of data from Gvoždík *et al.* (2010), based on their analysis of 16S and/or 12S rRNA genes in the area (see their supplementary materials).

Two different analyses of genetic structure were performed on the nuclear data. First, we applied

the Bayesian clustering algorithm of STRUCTURE (Pritchard *et al.*, 2000) to assign our 54 genotypes to K = 1–6 clusters, with three replicates per K, each consisting of 100 000 after a burnin of 10 000, using the admixture model with correlated allele frequency. For the K = 2 analysis, we report the ancestry coefficients to each cluster (Q_{sav} and Q_{fel}), which correspond to the two species (see Results). Second, we conducted a principal component analysis (PCA) on individual genotypes with the R packages *ade4* and *adegenet* (Jombart, 2008).

Niche modelling analysis

We used MaxEnt 3.3.3 (Phillips *et al.*, 2006, default settings) to predict high-quality potential distributions based on 509 known localities of *H. savignyi* and 136 known localities of *H. felixarabica* (Supporting Information, Table S2). We followed a similar procedure as in Dufresnes *et al.* (2018, see details therein), including (1) extraction of 23 bioclimatic and four landscape layers, (2) filtering of occurrences and exclusion of correlated variables with ENMTools 1.3 (Warren *et al.*, 2010), (3) assessment of model performance by computing the area under the curve (AUC), (4) computation of Schoener's D as a proxy for niche overlap, and (5) estimation of the relative contributions of each variable to the model. To generate Last Glacial Maximum (LGM) distributions, we applied two widely used general atmospheric circulation models: the Community Climate System Model (CCSM; http://www2.cesm.ucar.edu/) and the Model for Interdisciplinary Research on Climate (MIROC; Watanabe *et al.*, 2011). The area considered extended from 12° to 45°N and from 26° to 60°E, with spatial resolutions of 30 arc seconds (present) and 2.5 arc minutes (LGM).

The final dataset contained seven bioclimatic variables: Bio2 (mean diurnal range; °C × 10), Bio4 (temperature seasonality; standard deviation × 100), Bio8 (mean temperature of wettest quarter; °C × 10), Bio10 (mean temperature of warmest quarter; °C × 10), Bio 14 (precipitation of driest month; mm), Bio15 (precipitation seasonality; CV) and Bio19 (precipitation of coldest quarter, mm), along with nine other variables (Supporting Information, Table S3). The best-fit model was parameterized with a regularization multiplier of 1.0 for *H. savignyi* and 0.5 for *H. felixarabica* (30 replicates).

RESULTS

Genetic analyses

Our genomic data (1472 SNPs) distinguished the gene pools of *H. savignyi* and *H. felixarabica*, as seen from the STRUCTURE assignments (Fig. 1; K = 2, highest ΔK = 38 966.2) and the first axis of the PCA (61.5% of the genetic variance; Supporting Information, Fig. S1). Signs of introgression were weak for all three parapatric populations, i.e. loc. 3 (Q_{sav} = 0.91–0.94), loc. 4 (Q_{sav} = 0.95–0.98) and loc. 5 (Q_{fel} = 0.99–1.0), and completely absent in *H. felixarabica* populations from the southern part of the Rift, i.e. loc. 1–2 (Q_{fel} = 1.0), and *H. savignyi* populations from Cyprus, i.e. loc. 6–7 (Q_{sav} = 1.0) (Fig. 1). Moreover, the second axis of the PCA (7.3% of the genetic variance; Fig. S1) highlighted intraspecific structure within both species: between southern (loc. 1) and northern Levant (loc. 2, 5) in *H. felixarabica*; and between Cyprian (loc. 12–13) and continental (loc. 3–4) populations of *H. savignyi*.

The distributions of the mtDNA lineages of the two species are shown in Figure 1, and relationships between their 16S haplotypes are shown in Supporting Information Figure S2. There was no cyto-nuclear discordance: all individuals featured the mitotype that corresponds to their main nuclear ancestry (Fig. 1). We detected signs of genetic substructure within *H. felixarabica* between southern (Jordan, FEL5-8, FEL10-12) and northern populations (Lebanon, northern Israel and Syria, FEL09; also present in one sample from Jordan). In *H. savignyi*, we recovered the two main clades inhabiting the Levantine region (SAV15-29) and the rest of the range (SAV01-14), including private haplotypes on Cyprus (SAV01-03).

Niche modelling analyses

The MaxEnt models under current climate conditions had robust evaluation metrics for both species. The average test AUCs for the replicate runs was estimated as 0.947 (SD = 0.015) for *H. savignyi* and 0.988 (SD = 0.005) for *H. felixarabica*. Estimates of relative contributions of variables to the species are shown in Supporting Information Table S3. Niche overlap between *H. savignyi* and *H. felixarabica* was low (Schoener's D = 0.13). Predicted distributions under current and LGM conditions are shown in Figure 2. The Levant, and notably the parapatric ranges, have remained suitable for both species, especially during the LGM, where predicted distributions even appear to be wider (Fig. 2).

DISCUSSION

The tree frogs *H. savignyi* and *H. felixarabica* do not greatly admix along the Dead Sea Rift despite hundreds of kilometres of parapatry (Fig. 1). The limited introgression detected in our samples rather reflects old hybridization events. In addition, the absence of cyto-nuclear discordance indirectly argues for a geographically stable contact; moving hybrid

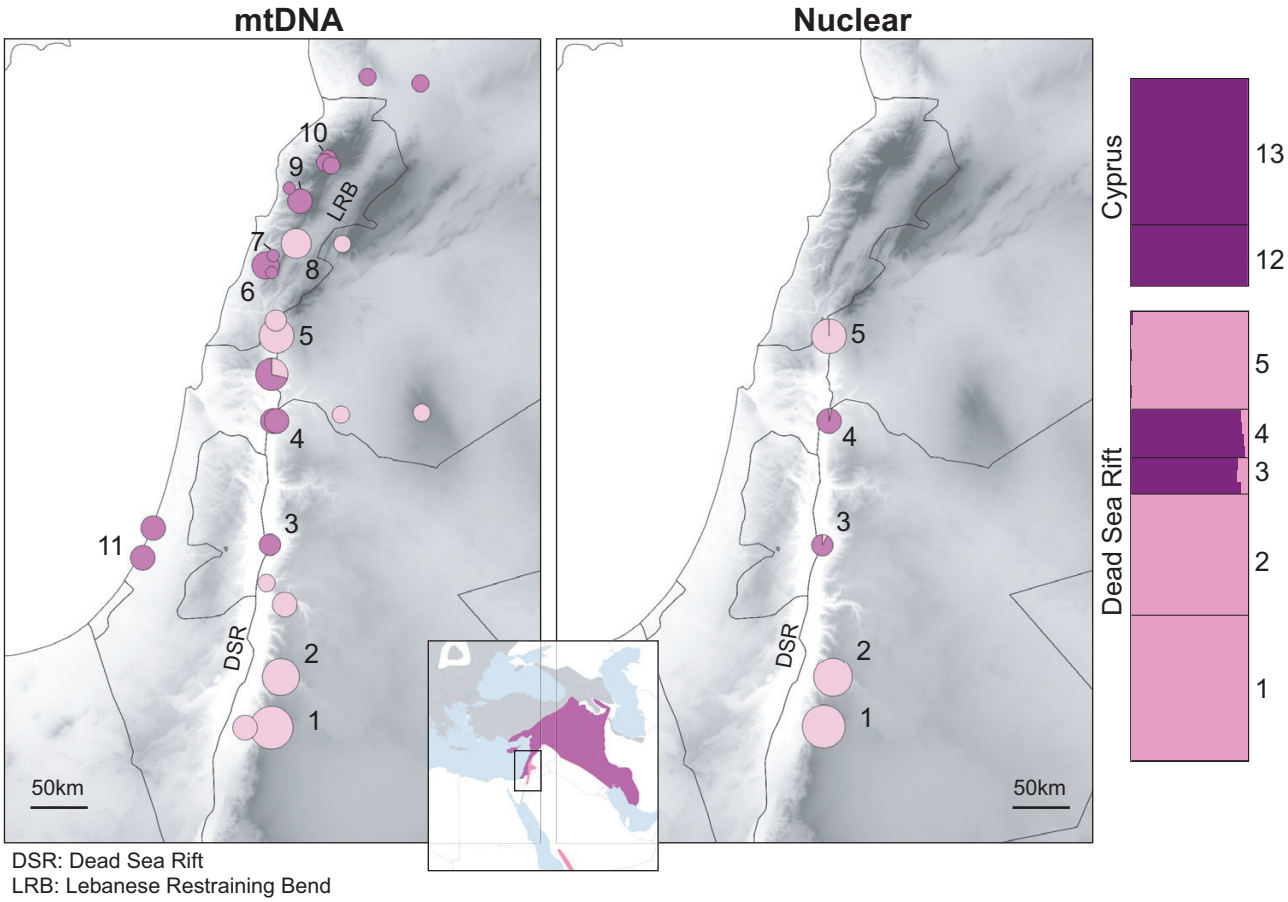

Figure 1. Distribution of the *Hyla savignyi* (purple) and *Hyla felixarabica* (pink) mitochondrial lineages (left, based on our samples and Gvoždík *et al.*, 2010) and nuclear gene pools (right, based on 1472 SNPs). Barplots show individual assignments. Localities 12 and 13 are reference *H. savignyi* populations from Cyprus.

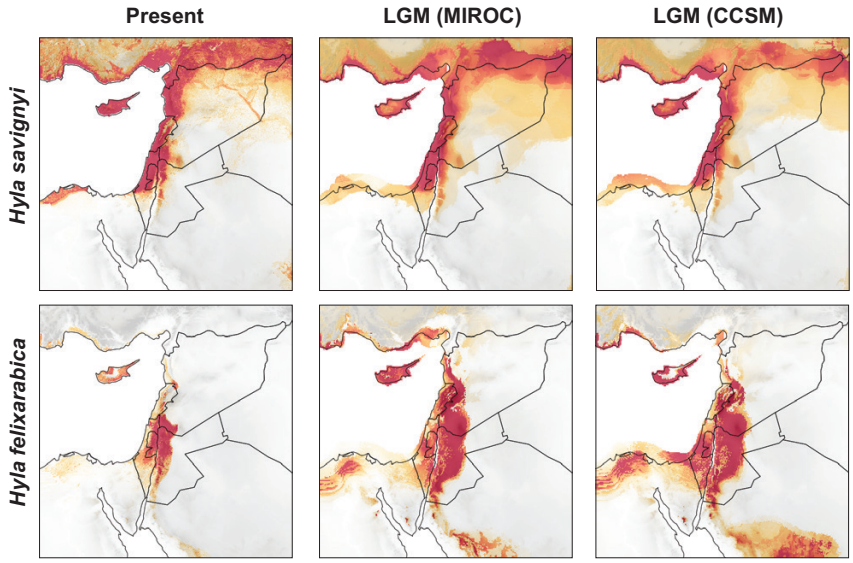

Figure 2. Species distribution models for *Hyla savignyi* (top row) and *Hyla felixarabica* (bottom row) under current conditions (left panels) and conditions during the Last Glacial Maximum (LGM, 21 000 years ago) under the MIROC (central panels) and CCSM models (right panels). Colour heat is proportional to the probability of occurrence.

zones that have not yet reached their equilibrium typically leave asymmetric traces of introgression (e.g. Wielstra *et al.*, 2017; van Riemsdijk *et al.*, 2019). It also suggests that mtDNA can be used as a reliable tool to map the distribution of these cryptic species (Gvoždík *et al.*, 2010). Based on 16S, we provide the first evidence of *H. felixarabica* in Lebanon, suggesting that its range follows the Dead Sea Rift also along the northern fault system, i.e. the Lebanese restraining bend (Fig. 1, loc. 8), reaching its northernmost limit at the Mount Lebanon massif (Fig. 1). Together, our analyses formally confirmed the distinction between *H. felixarabica* and *H. savignyi*, which were considered synonyms in some studies (Degani *et al.*, 2012).

What proximate mechanisms keep these two species on their respective sides of the Rift, and maintain their genetic integrity? From our niche modelling analyses, a transition of environmental conditions appears to be unlikely: the projected past and present distributions broadly encompass the southern Levant as a whole (Fig. 2). Despite little niche overlap (as expected given the very different realized ranges), both tree frogs are well adapted to Mediterranean environments (Dufresnes, 2019a), and could thus thrive throughout the region pending opportunities for dispersal (Fig. 2).

Therefore, difficulties crossing the Jordan Valley and/or incompatibilities between their diverged genomes are thus more plausible, non-mutually exclusive alternatives. Given their old divergence (Late Miocene, Dufresnes *et al.*, 2018), *H. savignyi* and *H. felixarabica* have probably reached an advanced stage of reproductive isolation, which is expected to translate into a narrow phylogeographical transition, even more so because their initial contact may pre-date the Holocene. Indeed, the modelled environmental conditions appear suitable for both species in the area of contact during the last glaciation (Fig. 2). LGM conditions similarly promoted range stability for several Middle Eastern terrestrial vertebrates during the Late Quaternary, supporting little dynamics of glacial retraction and post-glacial expansion (e.g. Javanbakht *et al.*, 2017; Vamberger *et al.*, 2017; Afroosheh *et al.*, 2019). The stable contact and putative reproductive isolation despite gene flow make *H. savignyi/felixarabica* a good candidate system to study whether and how pre-mating barriers evolved, for instance by comparing advertisement calls via bioacoustic surveys. Under a reinforcement scenario, we would expect increased inter-specific differences in the parapatric Rift populations than between populations far away from the contact.

In parallel, physical or ecological barriers could contribute to limit dispersal across the Jordan River and its barren valley. Major rivers often shape the distributions of parapatric amphibians at the micro-geographical scale. For instance, prehistoric shifts of the course of the Po in north-east Italy have triggered hybrid zone movement in *Bufotes* (Dufresnes *et al.*, 2014). In north-east Morocco, the Moulouyan valley mediates species transitions for many North African herpetofauna (Beddek *et al.*, 2018), including tree frog lineages (Dufresnes *et al.*, 2019a). Here the Dead Sea Rift could have isolated *H. savignyi* from *H. felixarabica* during the Late Pleistocene, when the Rift was filled by the palaeo-lake Lisan, the extensive ancestor of the present-day Dead Sea (Bartov *et al.*, 2007). However, today the brackish Jordan River is narrow (< 25 m in its lower parts) and flow is limited (Gafny *et al.*, 2010), thus making a weak barrier for amphibian dispersal. Instead, a shortage of breeding sites in the xeric surroundings of the river is a more likely cause of population isolation. The narrow Jordan Rift Valley (< 20 km wide) reaches several hundred metres below sea level and is famous for its desert climate and hypersaline lakes, with hot summers (> 40 °C) and very low rainfall (<< 300 mm/year) compared to immediately adjacent areas (> 500 mm/year; http://www.ims.gov.il/IMSEng/Tazpiot/RainObservations/). As a consequence, ephemeral pools and streams necessary for breeding are scarce and last only for a short period, making them unsuitable to complete larval development. Accordingly, a national survey of Israeli rain pools did not report *Hyla* tadpoles in the vicinity of the Rift, especially south of the Dead Sea (Goren & Milstein, 2017). In Lebanon, the transition could be further mediated by topographic barriers, e.g. Mount Lebanon massif, as suggested by the mitochondrial distributions.

While the Dead Sea Rift significantly affected the phylogeography of *Hyla*, whether it played a similar role in other species group is of debate. In the Eurasian blindsnake (*Xerotyphlops vermicularis*), an endemic lineage inhabits the eastern side of the Rift (Kornilios *et al.*, 2012; Kornilios, 2017), but western populations were not investigated. The opposite is found in *Rhynchocalamus* snakes, which feature an endemic species (*R. dayanae*) restricted to the western side, in southern Israel (Tamar *et al.*, 2016). The Levantine lizards *Phoenicolacerta kulzeri* and *P. laevis* show mosaic distributions, which seems to partially follow the catchment basins of the Jordan River, but only along some sections (Tamar *et al.*, 2015). Several species show no diversification within the region, and the Rift area rather corresponds to the eastern boundaries of their Levantine ranges (e.g. *Crocidura* shrews, Dubey *et al.*, 2007; *Ommatotrion vittatus*, van Riemsdijk *et al.*, 2017; *Testudo graeca terrestris*, Javanbakht *et al.*, 2017; *Pseudopus apodus*, Jandzik *et al.*, 2018; *Pelobates syriacus syriacus*, Dufresnes *et al.*, 2019b). Extensive hydrographic networks reportedly connected the Mediterranean coast to the Jordan Valley and perhaps even further eastwards during the Pleistocene, providing historical

colonization routes for water-associated organisms throughout the area (Heller, 2007).

Therefore, the phylogeographical transition observed in *Hyla* is an exception rather than a rule, one that may only apply to species pairs that diverged between the Levant and another biogeographical area, i.e. not *within* the Levant. It is plausible that desertification of the Arabian Peninsula (not the Dead Sea Rift) isolated *H. savignyi* and *H. felixarabica* during the Late Miocene, and that the latter species made it back to the Levant some time during the Pleistocene (2.0 Mya given Levant–Yemen mitochondrial sequence divergence, Gvoždík *et al.*, 2010; Dufresnes *et al.*, 2018). According to this scenario, the Dead Sea Rift would not be the initial driver of the *H. savignyi/felixarabica* split, but the geographical feature that later kept the resulting lineages apart, further promoting their divergence. Testing this scenario will require similar assessment in other vertebrates present in both the Levant and the Arabian Peninsula, such as *Bufotes* green toads and *Pelophylax* water frogs.

Future comparative surveys would benefit from international collaborations in this politically divided part of the world. Nature research and conservation activities can be ways to open dialogue across conflict zones, especially in the Middle East (Roulin *et al.*, 2017). In the wake of ongoing conservation actions bringing Israel closer to the Palestine authorities (e.g. EcoPeace Middle East, http://ecopeaceme.org/) as well as between the four countries sharing the Gulf of Aqaba (Krueger *et al.*, 2017), we encourage similar 'research for peace' efforts to gain better knowledge of the Dead Sea Rift biotic assemblages. As an overlooked phylogeographical border for amphibians, but a sensitive political border between Israel and the Arab world, the rift provides an iconic illustration of the cultural and faunal diversity of the Levant.

ACKNOWLEDGEMENTS

We thank Professors G. Degani and S. Gafny for providing samples from Israel, as well as D. Gruľa and P. Papežík for their help with the field and laboratory work. We also thank E. Geffen and S. Gafny for useful feedback on the manuscript. This study was funded by a grant from the Swiss National Science Foundation (31003A_166323) to Nicolas Perrin, and we are grateful for his support. D.J. was supported by the Slovak Research and Development Agency under contract no. APVV-15-0147.

REFERENCES

Afroosheh M, **Rödder D**, **Mikulicek P**, **Akmali V**, **Vaissi S**, **Fleck J**, **Schneider W**, **Sharifi M. 2019.** Mitochondrial DNA variation and Quaternary range dynamics in the endangered Yellow Spotted Mountain Newt, *Neurergus derjugini* (Caudata, Salamandridae). *Journal of Zoological Systematics and Evolutionary Research* **2019:** 1–11.

Ahmadzadeh F, **Flecks M**, **Rödder D**, **Böhme W**, **Ilgaz C**, **Harris DJ**, **Engler JO**, **Uzum N**, **Carretero MA. 2013.** Multiple dispersal out of Anatolia: biogeography and evolution of oriental green lizards. *Biological Journal of the Linnean Society* **110:** 398–408.

Baier F, Schmitz A, Sauer-Gürth H, Wink M. 2017. Pre-Quaternary divergence and subsequent radiation explain longitudinal patterns of genetic and morphological variation in the striped skink, Heremites vittatus. *BMC Evolutionary Biology* **17:** 132.

Bartov Y, **Enzel Y**, **Porat N**, **Stein M. 2007.** Evolution of the Late Pleistocene–Holocene Dead Sea basin from sequence statigraphy of fan deltas and lake-level reconstruction. *Journal of Sedimentary Research* **77:** 680–692.

Beddek M, **Zenboudji-Beddek S**, **Géniez P**, **Fathalla R**, **Sourouille P**, **Arnal V**, **Dellaoui B**, **Koudache F**, **Telailia S**, **Peyre O**, **Crochet P-A. 2018.** Comparative phylogeography of amphibians and reptiles in Algeria suggest common causes for the east-west phylogeographic breaks in the Maghreb. *PLoS ONE* **13**, e0201218.

Biton R, **Geffen E**, **Vences M**, **Cohen O**, **Bailon S**, **Rabinovich R**, **Malka Y**, **Oron T**, **Boistel R**, **Brumfeld V**, **Gafny S. 2013.** The rediscovered Hula painted frog is a living fossil. *Nature Communication* **4:** 1959.

Breslford A, **Dufresnes C**, **Perrin N. 2016.** High-density sex-specific linkage maps of European tree frog (*Hyla arborea*) identify the sex chromosome without information on offspring sex. *Heredity* **116:** 177–181.

Catchen J, **Hohenlohe P**, **Bassham S**, **Amores A**, **Cresko W. 2013.** Stacks: an analysis tool set for population genomics. *Molecular Ecology* **22:** 3124–3140.

Clement M, **Posada D**, **Crandall KA. 2000.** TCS: a computer program to estimate gene genealogies. *Molecular Ecology Notes* **9:** 1657–1659.

Degani G, **Nagar R**, **Yom-Din S. 2012.** Molecular DNA variation in *Hyla felixarabica* from various breeding sites in northern Israel. *Herpetologica Romanica* **6:** 51–67.

Dubey S, **Cosson J-F**, **Magnanou E**, **Vohralik V**, **Benda P**, **Frynta D**, **Hutterer R**, **Vogel V**, **Vogel P. 2007.** Mediterranean populations of the lesser white-toothed shrew (*Crocidura suaveolens* group): an unexpected puzzle of Pleistocene survivors and prehistoric introductions. *Molecular Ecology* **16:** 3438–3452.

Dufresnes C. 2019. *Amphibians of Europe, North Africa and the Middle East.* Campbell J, ed. London: Bloomsbury, 224.

Dufresnes C, **Beddek M**, **Skorinov DV**, **Fumagalli L**, **Perrin N**, **Crochet P-A**, **Litvinchuk SN. 2019a.** Diversification and speciation in tree frogs from the Maghreb (*Hyla meridionalis* sensu lato) with description of a new African endemic. *Molecular Phylogenetics and Evolution* **134:** 291–299.

Dufresnes C, **Bonato L**, **Novarini N**, **Betto-Colliard C**, **Perrin N**, **Stöck M. 2014.** Inferring the degree of incipient speciation in secondary contact zones of closely related

lineages of Palearctic green toads (*Bufo viridis* subgroup). *Heredity* **113:** 9–20.

Dufresnes C, **Mazepa G**, **Rodrigues R**, **Brelsford A**, **Litvinchuk SN**, **Sermier R**, **Betto-Colliard C**, **Blaser O**, **Borzée A**, **Cavoto E**, **Fabre G**, **Ghali K**, **Grossen C**, **Horn A**, **Lavanchy G**, **Leuenberger J**, **Phillips BC**, **Saunders PA**, **Savary R**, **Maddalena T**, **Stöck M**, **Dubey S**, **Canestrelli D**, **Jeffries DL. 2018.** Genomic evidence for cryptic speciation in tree frogs from the Apennine Peninsula, with description of *Hyla perrini* sp. nov. *Frontiers in Ecology & Evolution* **6:** 144.

Dufresnes C, **Strachinis I**, **Suriadna N**, **Mykytynets G**, **Cogălniceanu D**, **Székely P**, **Vukov T**, **Arntzen JW**, **Wielstra B**, **Lymberakis P**, **Geffen E**, **Gafny S**, **Kumlutaş Y**, **Ilgaz C**, **Candan K**, **Mizsei E**, **Szabolcs M**, **Kolenda K**, **Smirnov N**, **Geniez P**, **Lukanov S**, **Crottini A**, **Crochet P-A**, **Dubey S**, **Perrin N**, **Litvinchuk SN**, **Denoël M. 2019b.** Phylogeography of a cryptic speciation continuum in Eurasian spadefoot toads (*Pelobates*). *Molecular Ecology* (in press).

Guidon S, **Dufayard JF**, **Lefort V**, **Anisimova M**, **Hordijk W**, **Gascuel O. 2010.** PhyML 3.0: new algorithms, methods and utilities. *Systematic Biology* **59:** 307–321.

Gafny S, **Talozi S**, **Al Sheikh B**, **Ya'ari E. 2010.** Towards a living Jordan River: an environmental flow report on the rehabilitation of the Lower Jordan River. *EcoPeace / Friends of the Earth Middle East*. Available at: http://ecopeaceme.org/publications/publications/lower-jordan-river/.

Goren L, **Milstein D. 2017.** *Survey of amphibians in rain pools across Israel*. Science Division, Israel Nature and Parks Authority. Available at: https://www.parks.org.il/wp-content/uploads/2018/03/2017.pdf.

Gvoždík V, **Moravec J**, **Klütsch C**, **Kotlik P. 2010.** Phylogeography of the Middle Eastern tree frogs (*Hyla*, Hylidae, Amphibia) inferred from nuclear and mitochondrial DNA variation, with a description of a new species. *Molecular Phylogenetics and Evolution* **55:** 1146–1166.

Heller J. 2007. A historic biogeography of the aquatic fauna of the Levant. *Biological Journal of the Linnean Society* **92:** 625–639.

Hewitt GM. 2011. Quaternary phylogeography: the roots of hybrid zones. *Genetica* **139:** 617–638.

Jandzik D, **Jablonski D**; **Zinenko O**, **Kukushkin OV**, **Moravec J**, **Gvoždík V. 2018.** Pleistocene extinctions and recent expansions in an anguid lizard of the genus *Pseudopus*. *Zoologica Scripta* **47:** 21–32.

Javanebakht H, **Ihlow F**, **Jablonski D**, **Siroky P**, **Fritz U**, **Rödder D**, **Sharifi M**, **Mikulicek P. 2017.** Genetic diversity and Quaternary range dynamics in Iranian and Transcaucasian tortoises. *Biological Journal of the Linnean Society* **121:** 267–2640.

Jombart T. 2008. adegenet: a R package for the multivariate analysis of genetic markers. *Bioinformatics* **24:** 1403–1405.

Kornilios P. 2017. Polytomies, signal and noise: revisiting the mitochondrial phylogeny and phylogeography of the Eurasian blindsnake species complex (Typhlopidae, Squamata). *Zoologica Scripta* **46:** 665–674.

Kornilios P, **Ilgaz C**, **Kumlutas Y**, **Lymberakis P**, **Moravec J**, **Sindaco R**, **Rastegar-Pouyani N**, **Afroosheh M**, **Giokas S**, **Fraguedakis-Tsolis S**, **Chondropoulos B. 2012.** Neogene climatic oscillations shape the biogeography and evolutionary history of the Eurasian blindsnake. *Molecular Phylogenetics and Evolution* **62:** 856–873.

Krueger T, **Horwitz N**, **Bodin J**, **Giovani ME**, **Escrig S**, **Meibom A**, **Fine M. 2017.** Common reef-building coral in the Northern Red Sea resistant to elevated temperature and acidification. *Royal Society Open Science* **4:** 170038.

Phillips S, **Anderson R**, **Schapire R. 2006.** Maximum entropy modeling of species geographic distributions. *Ecological Modelling* **190:** 231–259.

Poulakakis N, **Paschalia K**, **Kardamaki A**, **Skourtanioti E**, **Gocmen B**, **Ilgaz C**, **Kumlutas Y**, **Avci A**, **Lymberakis P. 2013.** Comparative phylogeography of six herpetofauna species in Cyprus: late Miocene to Pleistocene colonization routes. *Biological Journal of the Linnean Society* **108:** 619–635.

Pritchard JK, **Stephens M**, **Donnelly P. 2000.** Inference of population structure using multilocus genotype data. *Genetics* **155:** 945–959.

Remington CL. 1968. Suture-zones of hybrid interaction between recently joined biotas. In: Dobzhansky T, Hecht MK, Steere WC, eds. *Evolutionary biology*. New York: Plenum Press, 321–428.

van Riemsdijk I, **Arntzen JW**, **Bogaerts S**, **Franzen M**, **Litvinchuk SN**, **Olgun K**, **Wielstra B. 2017.** The Near East as a cradle of biodiversity: a phylogeography of banded newts (genus *Ommatotriton*) reveals extensive inter- and intraspecific genetic differentiation. *Molecular Phylogenetics and Evolution* **114:** 73–81.

van Riemsdijk I, **Butlin RK**, **Wielstra B**, **Arntzen JW. 2019.** Testing an hypothesis of hybrid movement for toads in France. *Molecular Ecology* 28: 1070–1083.

Roulin A, **Rashid A**, **Spiegel B**, **Charter M**, **Dreiss AN**, **Leshem Y. 2017.** 'Nature knows no boundaries': the role of nature conservation in peacebuilding. *Trends in Ecology and Evolution* **32:** 305–310.

Schuster M, **Duringer P**, **Ghienne J-F**, **Vignaud P**, **Mackaye HT**, **Likius A**, **Brunet M. 2006.** The age of the Sahara desert. *Science* **311:** 821.

Tamar K, **Carranza S**, **In den Bosh H**, **Sindaco R**, **Moravec J**, **Meiri S. 2015.** Hidden relationships and genetic diversity: molecular phylogeny and phylogeography of the Levantine lizards of the genus *Phoenicolacerta* (Squamata: Lacertidae). *Molecular Phylogenetics and Evolution* **91:** 86–97.

Tamar K, **Šmíd J**, **Göçmen B**, **Meiri S**, **Carranza S. 2016.** An integrative systematic revision and biogeography of *Rhynchocalamus* snakes (Reptilia, Colubridae) with a description of a new species from Israel. *PeerJ* **4:** e2769.

Vamberger M, **Stuckas H**, **Vargas-Ramirez M**, **Kehlmaier C**, **Ayaz D**, **Aloufi AA**, **Lymberakis P**, **Siroky P**, **Fritz U. 2017.** Unexpected hybridization patterns in Near Eastern terrapins (*Mauremys caspica*, *M. rivulata*) indicate ancient gene flow across the Fertile Crescent. *Zoologica Scripta* **46:** 401–4013.

Warren DL, **Glor RE**, **Turelli M. 2010.** ENMTOOLS: a toolbox for comparative studies of environmental niche models. *Ecography* **33:** 607–611.

Watanabe S, **Hajima T**, **Sudo K**, **Nagashima T**, **Takemura H**, **Okajima H**, **Nozawa T**, **Kawase H**, **Abe M**, **Yokohata T**, **Ise T**, **Sato H**, **Kato E**, **Takata K**, **Emori S**, **Kawamiya M. 2011.** MIROC-ESM 2010: model description and basic results of CMIP5-20c3m experiments. *Geoscientific Model Development* **4:** 845–872.

Wielstra B, **Burke T**, **Butlin RK**, **Avcı A**, **Üzüm N**, **Bozkurt E**, **Olgun K**, **Arntzen JW. 2017.** A genomic footprint of hybrid zone movement in crested newts. *Evolution Letters* **2:** 93–101.

SUPPORTING INFORMATION

Additional Supporting Information may be found in the online version of this article at the publisher's website.

Table S1. Details on the samples included in this study.
Table S2. Locality information used to build the species ecological niche.
Table S3. Relative contributions of the variables in the Maxent models.
Figure S1. PCA on individual RAD genotypes.
Figure S2. Phylogeny and haplotype network of our 16S sequences.

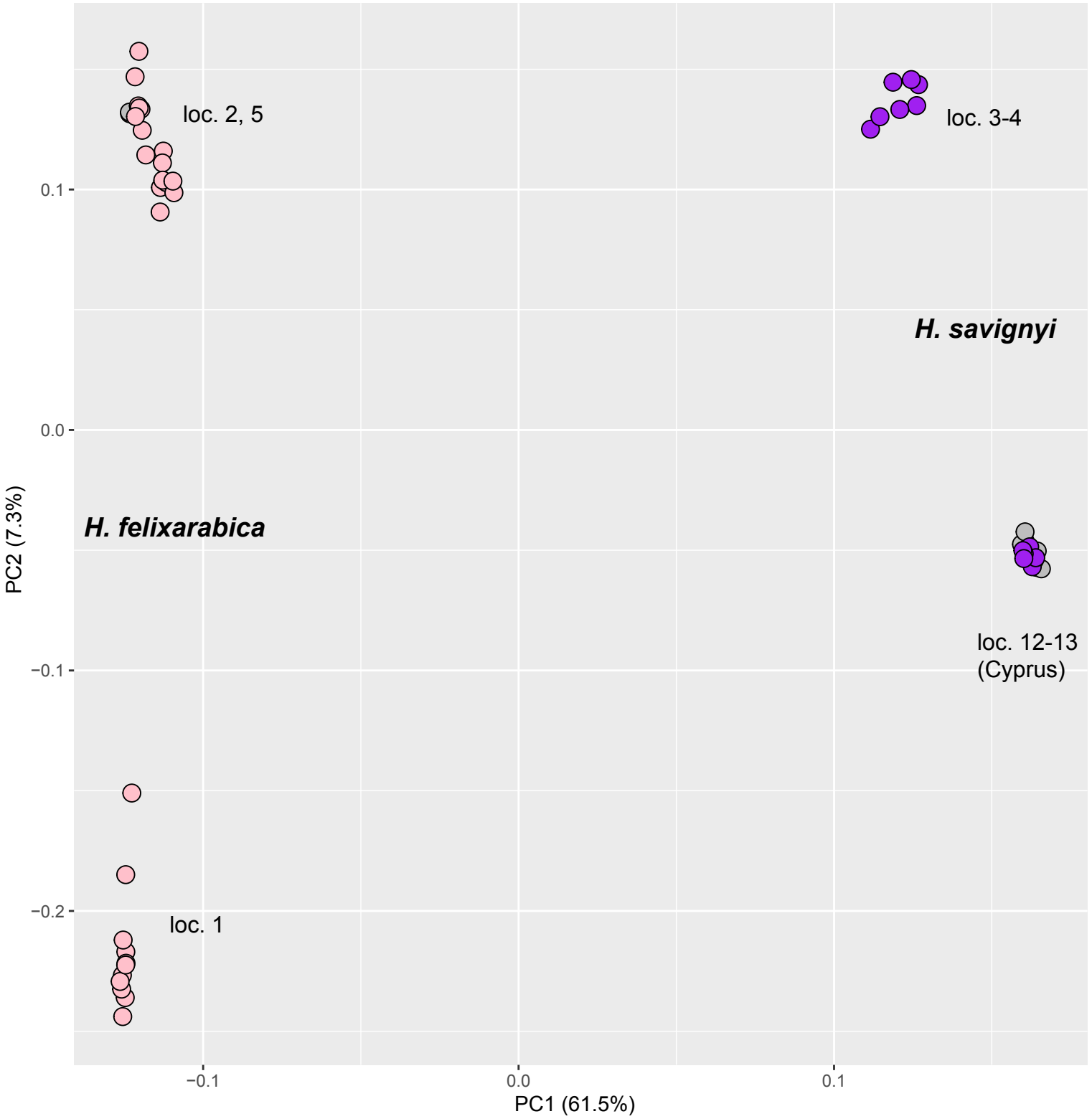

Fig. S1: Principal Component Analysis (PCA) on individual genotypes, based on 1,472 SNPs. Colors indicate the mitochondrial identity of samples (purple: *H. savignyi*; pink: *H. felixarabica*; grey: not mitotyped).

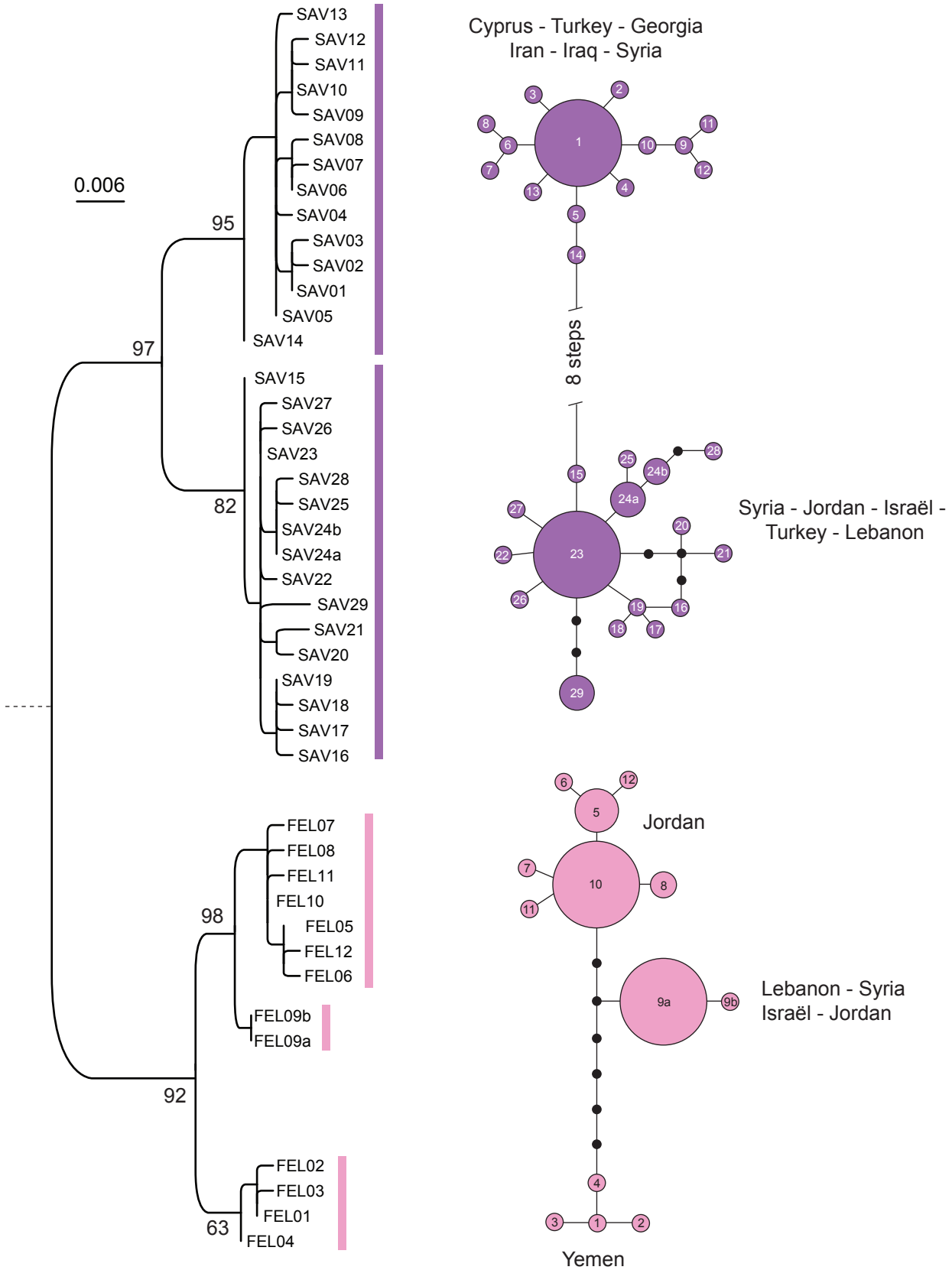

Fig. S2: Maximum-Likelihood phylogeny and haplotype networks of *H. savignyi* and *H. felixarabica* 16S haplotypes, combining our sequences with those from Gvozdik et al. (2010). Branch supports are indicated for the major branches (out of 1,000 bootstrap replicates). Haplotype numbers are indicated within the circles.

Table S1: Details on the samples of this study, including their origin, 16S haplotypes (corresponding to Fig. S2), and nuclear ancestry coefficients to the *H. felixarabica* (Q_{fel}) or *H. savignyi* (Q_{sav}) nuclear cluster, as inferred from the RAD data.

Loc.	Sample	Country	Locality	Latitude	Longitude	Sex	16S	Q_{fel}	Q_{sav}
1	SL.355	Jordan	Canyon S Dana	30.650	35.600	M	FEL08	1.00	0.00
1	SL.356	Jordan	Canyon S Dana	30.650	35.600	M	FEL10	1.00	0.00
1	SL.357	Jordan	Canyon S Dana	30.650	35.600	M	FEL10	1.00	0.00
1	SL.359	Jordan	Canyon S Dana	30.650	35.600	M	FEL10	1.00	0.00
1	SL.360	Jordan	Canyon S Dana	30.650	35.600	M	FEL10	1.00	0.00
1	SL.361	Jordan	Canyon S Dana	30.650	35.600	M	FEL10	1.00	0.00
1	SL.362	Jordan	Canyon S Dana	30.650	35.600	M	FEL10	1.00	0.00
1	SL.363	Jordan	Canyon S Dana	30.650	35.600	M	FEL10	1.00	0.00
1	SL.364	Jordan	Canyon S Dana	30.650	35.600	M	FEL10	1.00	0.00
1	SL.382	Jordan	Canyon S Dana	30.650	35.600	M	FEL10	1.00	0.00
1	SL.381	Jordan	Canyon S Dana	30.650	35.600	M	FEL11	1.00	0.00
1	SL.358	Jordan	Canjon S Dana	30.650	35.600	M	FEL12	1.00	0.00
2	SL.348	Jordan	wadi Hassa	30.974	35.671	M	-	1.00	0.00
2	SL.350	Jordan	wadi Hassa	30.974	35.671	M	FEL05	1.00	0.00
2	SL.351	Jordan	wadi Hassa	30.974	35.671	M	FEL05	1.00	0.00
2	SL.352	Jordan	wadi Hassa	30.974	35.671	M	FEL05	1.00	0.00
2	SL.353	Jordan	wadi Hassa	30.974	35.671	M	FEL06	1.00	0.00
2	SL.354	Jordan	wadi Hassa	30.974	35.671	M	FEL07	1.00	0.00
2	SL.347	Jordan	wadi Hassa	30.974	35.671	M	FEL09a	1.00	0.00
2	SL.067	Jordan	wadi Hassa	30.974	35.671	M	FEL10	1.00	0.00
2	SL.280	Jordan	wadi Hassa	30.974	35.671	M	FEL10	1.00	0.00
2	SL.349	Jordan	wadi Hassa	30.974	35.671	M	FEL10	1.00	0.00
3	SL.068	Jordan	Jordan River	31.823	35.585	M	SAV23	0.06	0.94
3	SL.093	Jordan	Jordan River	31.823	35.585	M	SAV23	0.08	0.92
3	SL.092	Jordan	Jordan River	31.823	35.585	M	SAV23	0.09	0.91
4	SL.058	Jordan	Al shouna Al Shamaliya	32.609	35.637	M	SAV23	0.03	0.98
4	SL.060	Jordan	Al shouna Al Shamaliya	32.609	35.637	M	SAV23	0.04	0.96
4	SL.059	Jordan	Al shouna Al Shamaliya	32.609	35.637	M	SAV24b	0.03	0.97
4	SL.061	Jordan	Al shouna Al Shamaliya	32.609	35.637	M	SAV24b	0.05	0.95
5	SL. L8	Israel	Lehavot	33.152	35.638	larvae	FEL09a	0.99	0.01
5	SL. L2	Israel	Lehavot	33.152	35.638	larvae	FEL09a	0.99	0.01
5	SL. L5	Israel	Lehavot	33.152	35.638	larvae	FEL09a	0.99	0.01
5	SL. L1	Israel	Lehavot	33.152	35.638	larvae	FEL09a	1.00	0.00
5	SL. L3	Israel	Lehavot	33.152	35.638	larvae	FEL09a	1.00	0.00
5	SL. L4	Israel	Lehavot	33.152	35.638	larvae	FEL09a	1.00	0.00
5	SL. L6	Israel	Lehavot	33.152	35.638	larvae	FEL09a	1.00	0.00
5	SL. L7	Israel	Lehavot	33.152	35.638	larvae	FEL09a	1.00	0.00
6	DJ6740	Lebanon	Salima	33.594	35.555	M	SAV23	-	-
6	DJ6741	Lebanon	Salima	33.594	35.555	M	SAV23	-	-
6	DJ6738	Lebanon	Salima	33.594	35.555	M	SAV28	-	-
6	DJ6737	Lebanon	Salima	33.594	35.555	M	SAV	-	-
6	DJ6739	Lebanon	Salima	33.594	35.555	M	SAV	-	-
7	DJ6789	Lebanon	Moukhtara	33.657	35.609	M	SAV23	-	-
8	DJ6770	Lebanon	Houch El Saalouk	33.732	35.785	F	FEL09a	-	-
8	DJ6771	Lebanon	Houch El Saalouk	33.732	35.785	M	FEL09a	-	-
8	DJ6772	Lebanon	Houch El Saalouk	33.732	35.785	F	FEL09a	-	-
8	DJ6773	Lebanon	Houch El Saalouk	33.732	35.785	F	FEL09a	-	-
8	DJ6774	Lebanon	Houch El Saalouk	33.732	35.785	F	FEL09a	-	-
8	DJ6775	Lebanon	Houch El Saalouk	33.732	35.785	M	FEL09a	-	-

Table S1 (continued)

Loc.	Sample	Country	Locality	Latitude	Longitue	Sex	16S	Q_{fel}	Q_{sav}
9	DJ6800	Lebanon	Faqra	33.998	35.813	-	SAV23	-	-
9	DJ6799	Lebanon	Faqra	33.998	35.813	-	SAV29	-	-
9	DJ6801	Lebanon	Faqra	33.998	35.813	F	SAV29	-	-
9	DJ6802	Lebanon	Faqra	33.998	35.813	M	SAV29	-	-
10	DJ6834	Lebanon	Ariz	34.261	36.023	M	SAV23	-	-
10	DJ6835	Lebanon	Ariz	34.261	36.023	M	SAV23	-	-
11	CQ.83	Israel	Robert's pool	31.740	34.630	larvae	SAV23	-	-
11	CQ.85	Israel	Robert's pool	31.740	34.630	larvae	SAV23	-	-
11	CQ.84	Israel	Robert's pool	31.740	34.630	larvae	SAV24	-	-
11	CQ.86	Israel	Robert's pool	31.740	34.630	larvae	SAV24	-	-
12	SL.365	Cyprus	Amathus	34.717	33.133	M	SAV01	0.00	1.00
12	SL.366	Cyprus	Amathus	34.717	33.133	M	SAV01	0.00	1.00
12	SL.367	Cyprus	Amathus	34.717	33.133	F	SAV01	0.00	1.00
12	SL.383	Cyprus	Amathus	34.717	33.133	F	SAV01	0.00	1.00
12	SL.384	Cyprus	Amathus	34.717	33.133	M	SAV01	0.00	1.00
13	SL.368	Cyprus	Finikaria	34.750	33.083	F	SAV01	0.00	1.00
13	SL.369	Cyprus	Finikaria	34.750	33.083	M	SAV01	0.00	1.00
13	SL.370	Cyprus	Finikaria	34.750	33.083	M	SAV01	0.00	1.00
13	SL.371	Cyprus	Finikaria	34.750	33.083	M	SAV01	0.00	1.00
13	SL.372	Cyprus	Finikaria	34.750	33.083	M	SAV01	0.00	1.00
13	SL.385	Cyprus	Finikaria	34.750	33.083	F	SAV01	0.00	1.00
13	SL.373	Cyprus	Finikaria	34.750	33.083	M	-	0.00	1.00
13	SL.374	Cyprus	Finikaria	34.750	33.083	M	-	0.00	1.00
13	SL.375	Cyprus	Finikaria	34.750	33.083	M	-	0.00	1.00
13	SL.376	Cyprus	Finikaria	34.750	33.083	F	-	0.00	1.00
13	SL.377	Cyprus	Finikaria	34.750	33.083	M	-	0.00	1.00
13	SL.378	Cyprus	Finikaria	34.750	33.083	F	-	0.00	1.00
14	DJ8163	Cyprus	Episkopi	34.800	32.529	F	SAV01	-	-

Table S3: Relative contribution of variables for the present time MaxEnt models for *Hyla savignyi* and *H. felixarabica*, estimated from jackknife analyses.

Variable	Percent of contribution	
	H. savignyi	*H. felixarabica*
Altitude	0.4	4.0
Aridity index	6.4	13.0
Aspect	0.2	0.4
Exposition	0.1	0
Habitat homogenity	29.3	12.7
Land cover	1.8	0.2
Mean diurnal range (Bio 2)	0.4	1.7
Mean temperature of warmest quarter (Bio 10)	8.3	2.5
Mean temperature of wettest quarter (Bio 8)	11.1	10.5
Precipitation of driest month (Bio 14)	2.8	1.3
Precipitation seasonality (Bio 15)	4.0	10.1
Precipitation of coldest quarter (Bio 19)	29.1	6.3
Slope	0	0.7
Temperature seasonality (Bio 4)	1.8	34.6
Terrain roughness index	0	0.1
Tree coverage percent	4.2	1.9